NEOCLASSICAL TRANSPORT IN THE W VII-AS STELLARATOR

H.Maassberg, U. Gasparino, G. Kühner, H. Ringler
W VII-AS Team* and NI Team**
Max-Planck Institut für Plasmaphysik
Association EURATOM-IPP, D-8046 Garching, FRG
ECRH Group†
Institut für Plasmaforschung der Universität Stuttgart
D-7000 Stuttgart, FRG

Abstract

For the rather complex magnetic field topology of W VII-AS stellarator, the full neoclassical transport matrix with radial electric field included in both the plateau and long mean free path regime is calculated using the DKES code. The toroidal resonance for larger radial electric fields is found to be important for the ion transport coefficients with up to seven roots of the ambipolarity condition in the LMFP regime. Temperature and density profiles measured by Thomson scattering for the first ECF heated discharges (at 2^{nd} harmonic) are analysed, the electron heat conduction coefficient is estimated and compared with the neoclassical prediction.

Introduction

The new W VII-AS stellarator is characterized by a rather complex magnetic field topology /1/. The representation of magnetic field strength on flux surfaces, which determines the neoclassical transport properties, leads to a very large number of Fourier coefficients in magnetic flux coordinates. In Figure 1 the $|\mathbf{B}|$-contours for approximately half minor radius are plotted. The particles trapped in the absolute minimum, B_{min}, contribute significantly to the neoclassical transport in long mean free path (LMFP) regime, more than 20 Fourier coefficients in the $|\mathbf{B}|$-representation are necessary (e.g., with only 7 Fourier coefficients, the particle transport coefficient is decreased by a factor of about 2). Consequently, simple analytic estimates of the neoclassical transport coefficients are unqualified and a full numerical solution of the drift kinetic equation is used (DKES code /2/) to compute the full transport matrix.

After 2 months of plasma operation in the W VII-AS stellarator, the experimental database for analyzing the energy transport is only small. Up to now, electron density and temperature profiles from the Thomson scattering diagnostic are available for 2^{nd} harmonic ECF maintained discharges ($B_0 \approx 1.26$ T) with heating power up to 500 kW (3 gyrotrons) mainly at rotational transforms $\iota > 0.5$. For these conditions with moderate T_e, the electron collisionality is typically close to the plateau regime. In the LMFP-regime ($1/\nu$-regime), the neoclassical transport is expected to determine the experimental energy balance analogous as in HELIOTRON-E (/3/). Modeling the energy source and loss terms with regard to the experimental conditions, the energy balance equation is used to fit the electron temperature profile yielding the experimental electron heat conduction coefficient.

Neoclassical Transport Code

The DKES code (Drift Kinetic Equation Solver /2/) is based on the linearized monoenergetic drift kinetic equation in magnetic flux coordinates for each particle species with radial electric field included. As the poloidal component of the ∇B-drift is neglected, the solution depends only on the $|\mathbf{B}|$-Fourier spectrum independently for each magnetic surface. Typically, about 200 Fourier harmonics for both poloidal and toroidal angle and up to 150 Legendere polynomials in pitch angle are used to represent the neoclassical deviation of the distribution function from the Maxwellian. Especially in the LMFP with moderate radial electric fields, this large number of basis functions is necessary for the estimation of the non-diagonal term of the monoenergetic Onsager transport matrix. For each magnetic surface, the 3 monoenergetic transport coefficients are computed for varying collisionality and radial electric field (more than 200 values with up to 10 min. CPU on the CRAY 1 for each run). On this grid of storaged monoenergetic transport coefficients, the energy convolution is performed based on bi-cubic interpolation resulting in

* ** † see paper of Gasparino, U. et al., this conference

the full transport matrix D_{ij} which is slightly different defined with respect to the Onsager form (but more practical for an experimental environment):

$$\Gamma = -n \cdot \{D_{11}(\frac{n'}{n} + \frac{q\Phi'}{T}) + D_{12}\frac{T'}{T} + D_{13}E_{\|}\}$$

$$Q = -nT \cdot \{D_{21}(\frac{n'}{n} + \frac{q\Phi'}{T}) + D_{22}\frac{T'}{T} + D_{23}E_{\|}\}$$

$$j_{\|} = -\{D_{31}(\frac{n'}{n} + \frac{q\Phi'}{T}) + D_{32}\frac{T'}{T} + D_{33}E_{\|}\}$$

where Γ is the particle flux, Q the heat conduction, $j_{\|}$ the toroidal net current density, $\Phi' = -E_r$ the radial electric field and $'$ denotes the radial derivative (flux coordinate). For a fixed magnetic configuration (defined by rotational transform, ι, vertical field, B_z, and pressure profile, $\beta(r)$) the monoenergetic transport coefficients are computed for different minor radii, cubic interpolation in r is applied in connection with the energy convolution algorithm. For larger values of radial electric field, high resolution is necessary close to the toroidal resonance, $E_r = \iota v r B_0/R$, strongly affecting the ion transport coefficients in both the plateau and the LMFP regime. Due to this toroidal resonance, several roots of the ambipolarity condition (up to 7 values for radial electric field) can exist in the LMFP regime. In Figure 2, the electron and ion transport coefficients versus E_r are shown with a 2nd maximum in the ion transport coefficients at the toroidal resonance. This result is contrary to the simple picture of radial electric field based on the Shaing-Houlberg transport model /4/ (only 2 stable and 1 instable root possible). In general, however, with the condition of ambipolarity, the radial electric field, particle and energy flux and the bootstrap current can be calculated for a given density and temperature profile. First calculations indicate, that the neoclassical radial electric field is negative in the plateau regime (typical for NBI heated discharges) and can become positive in the LMFP regime (ECF heated discharges). For an axisymmetric field, DKES computations were compared with Monte Carlo simulations /5/, nearly identical particle and energy transport coefficients were found. Furthermore, the bootstrap coefficient, D_{31}, was tested using the relation to particle transport /6/, reliable agreement was found.

The particle and energy transport coefficients in the plateau regime are comparable to those of an equivalent axisymmetric case showing some improvement due to the advanced stellarator concept. In the W VII-AS configuration, however, the strong localized minimum in $|\mathbf{B}|$ (see Fig. 1) leads to a rather large fraction of trapped particles contributing significantly to the transport. An additional B_z-field affects this fraction of trapped particles and their radial drift. Calculations show, that an additional B_z-field of $\pm$ 300 G changes the neoclassical particle and energy transport coefficients by a factor of 2; the bootstrap current coefficients, however, are found to be nearly unaffected by the B_z-field. The electron energy transport coefficient, D_{22} (called heat conduction coefficient χ in the next section), is typically by a factor of 3 larger than the coefficient D_{21}. Furthermore, the density profiles are broader than the electron temperature profile justifying the diffusive ansatz for the heat conduction coefficient fit.

1st Estimates of Electron Heat Conduction

Electron density and temperature profiles are measured by the Thomson scattering diagnostic in a series of discharges similar as in the old W VII-A stellarator (a new single shot system is under construction). The quality and reliability of these profiles depends mainly on accurate control of all machine parameters (e.g. gas feed), but also on the stability of the discharges, in some cases, current control by a small loop voltage increases the reproducebility. Within a series, only discharges with nearly indentical values of line density and energy content are used. In future, also the ECE temperature measurements which are absolutely calibrated should be used to confirm the Thomson profile data. For estimating the electron heat conduction on the basis of the energy balance equation, the local power source and loss terms must be known. For the low density ($n_e < 3 \cdot 10^{13}\ cm^{-3}$) discharges with 2^{nd} harmonic ECF heating at $B_0 \approx 1.26$ T in the first 2 months of operation, the radiation losses and the collisional power transfer to the ions are rather small: each of the order of less than 35 kW. The experimental estimation of absorbed ECF power is deduced from ECE data after a gyrotron is switched off: the local power absorption is given by the transient decay of electron temperature. However, at 2^{nd} harmonic heating, only 7 radial ECE channels are available and the separation between ECF power deposition and the range with heat transport is not very reliable. Simulations of the switch off phase indicate, that the power deposition

range is limited to the inner ECE channels. However, the estimation of the total absorbed power (and ECF heating efficiency) is rather inaccurate. Consequently, we assume about 75% of gyrotron power being absorbed, this is consistent with single pass ray tracing calculations (nearly full absorption) and the ECE data. The deposition profile is mainly determined by the broadness (half witdh diameter about 3 cm), the distance of the ECF beam from the magnetic axis and the resonant magnetic field value: the power deposition profile is modeled by a shifted Gaussian (standard deviation $\sigma = 1.5$ cm) centered at at r_{abs} depending on the value of magnetic field on axis. The fit of the heat conduction coefficient based on energy balance depends only linear on the value of total absorbed power leading to an uncertainty of less than a factor of 2 for $r > r_{abs}$. The power loss terms are estimated by an average oxygen radiation model renormalized to the bolometry data and by the usual collisional power transfer to the plasma ions. Doing this, the power source model depends only slightly on the value of Z_{eff} which is rather unknown for this type of discharges. With this source model, the electron energy balance equation is integrated with the ansatz of a power series in normalized minor radius for the logarithm of the heat conduction coefficient, the coefficients of the power series are calculated by weighted least square fit to the electron temperature profile. For the electron density representation, a standard least square best fit is used.

The profiles (shots 185-206) in Figure 3 are the 1st Thomson series of W VII-AS stellarator measured at the 1st day of operation! The H_2 discharge heated with $P_{abs} \simeq 130$ kW with 1 gyrotron was not stable: the central density increases up to the cut-off limit. The time of the Thomson profile, however, was close to the maximum of the energy content. In this series, the ECF power was deposited in the center, at $\iota \simeq 0.53$ the outer part of the plasma radius was destroyed by natural islands related to $\iota = 5/9$. The profiles (He discarges in shots 906-923) shown in Figure 4 are more typical for the first two months: much broader temperature and density profiles, the ECF power was absorbed ($P_{abs} \approx 300$ kW with 2 gyrotrons) more outside. For both cases, the least square best fit of χ has an accuracy of about 50% within the gradient region of electron temperature mainly determined by the scattering of the Thomson data and the uncertainty of absorbed power. In the central part as well as at outer radii, the error is expected to be much larger. However, the best fit suppresses strong local changes in electron heat conduction and in the central part, due to the relative large experimental error bars of Fig. 4 which are used as weighting functions, χ^{ex} is mainly influenced by larger radii. For comparison, the neoclassical coefficients χ^{DKES} and χ^{H-H} based on the Hinton-Hazeltine model /7/ and the old W VII-A anomalous coefficient χ^{an} /8/ are also shown. In all analyzed profiles, χ^{ex} increases strongly at outer radii, but for some profiles also in the central part for very flat T_e profiles (tendency for even hollow $T_e(r)$). For most of the analyzed profiles, the agreement of χ^{ex} and χ^{an} is much better at outer radii than in the example of Fig. 4, but the ratio of χ^{ex} to χ^{DKES} is much larger than in the central part of Fig. 3. Furthermore, for the series in Fig. 4 a neoclassical bootstrap current of about 1 kA is expected from DKES code (for $Z_{eff} \simeq 3$), I_b is in reasonable agreement /9/ with the measured toroidal current.

Conclusions

The neoclassical transport in W VII-AS with the complex field structure is described using the DKES code, the full transport matrix is computed with radial electric fields included. For the discharges of the 1st two months of plasma operation with 2^{nd} harmonic ECF heating, the experimental values of the electron heat conduction coefficient are governed by anomalous transport. In this regime of plasma parameters, the heat conduction is larger than the neoclassical prediction.

References

/1/ J. Kisslinger, F. Rau and H. Wobig, Fusion Tech. (Proc. 12th Symp. 1982), Pergamon (1983), 1051
/2/ S.P. Hirshman et al., Phys. Fluids **29** (1986), 2951
/3/ T. Obiki et al., 12th Int. Conf. on Plasma Phys. and Contr. Nucl. Fus. (1988), IAEA-CN-50/C-1-1
/4/ K.C. Shaing et al., Plasma Phys. and Contr. Nucl. Fusion Res., **2**, IAEA Vienna (1984), 189
/5/ W. Lotz and J. Nührenberg, Phys. Fluids, **31** (1988), 2984
/6/ H. Wobig, Report **IPP 2/297** (1988)
/7/ F.L. Hinton and W.N.G. Hazeltine, Rev. Mod. Phys., **48** (1976), 239
/8/ G. Grieger et al., Plasma Phys. and Contr. Fusion, **28** No. 1A (1986), 43
/9/ U. Gasparino et al., this conference

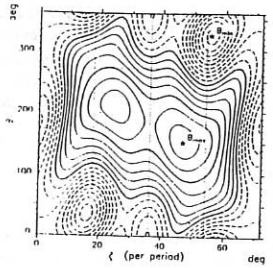

Fig. 1: $|\mathbf{B}|$ contours on magnetic flux surface: $r \simeq 10$ cm, $\iota \simeq 0.51$ (for vacuum field).

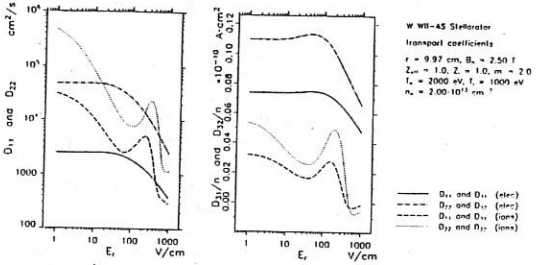

Fig. 2: Neoclassical Transport coefficients (DKES code) D_{11} and D_{22} (on the left) and D_{31} and D_{32} (on the right) versus radial electric field, E_r.

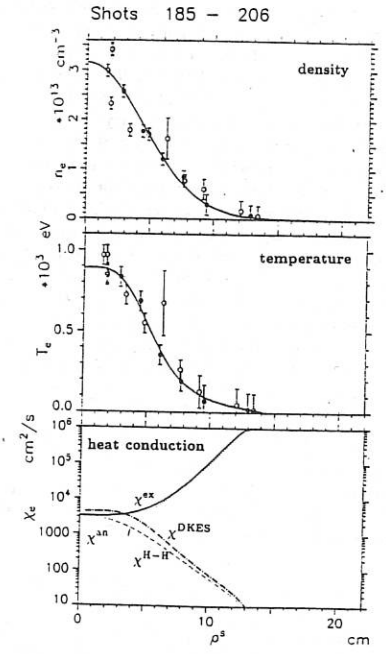

Fig. 3: $n_e(r)$ and $T_e(r)$ by Thomson scattering diagnostic and fit of electron heat conduction, $\chi(r)$, for H_2 discharge with $P_{abs} \simeq 130$ kW (1 gyrotron) at $r_{abs} \simeq 3$ cm ($B_0 \simeq 1.274$ T with resonance on axis).

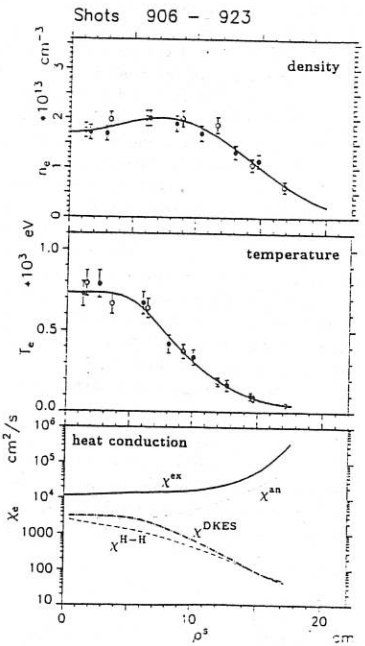

Fig. 4: $n_e(r)$ and $T_e(r)$ by Thomson scattering diagnostic and fit of electron heat conduction, $\chi(r)$, for He discharge with $P_{abs} \simeq 300$ kW (2 gyrotron) at $r_{abs} \simeq 5.5$ cm ($B_0 \simeq 1.256$ T with resonance shifted inside).